Electronic Supporting Information file for

Dual Solar-Driven Hydrogen Evolution and Alcohol Oxidation with CdS Quantum Dot-Sensitized Photocatalysis Prepared by SILAR Methodology

Vasilis Nikolaou,[†a] Deborah Romito,[†a] Clément Maheu,[b] Jonathan Hamon,[b] Eric Gautron,[b] Florian Massuyeau,[b] Pierre-Emmanuel Petit,[b] Stéphane Jobic,*[b] Fabrice Odobel*[a]

[a]*Nantes Université, CNRS, Chimie Et Interdisciplinarité Synthèse Analyse Modélisation, CEISAM, UMR 6230, F-44000 Nantes, France.*

[b]*Nantes Université, CNRS, Institut des Matériaux de Nantes Jean Rouxel, IMN, F-44000 Nantes, France*

*Correspondence to: *stephane.jobic@cnrs-imn.fr* and *fabrice.Odobel@univ-nantes.fr*

‡ These authors have equally contributed

Contents

Experimental section

Materials

All reagents were purchased from common commercial sources and used without any further purification, unless otherwise stated. The TiO_2 nanoparticles in this work are commercially available Titanium(IV) oxide – nanopowder, 21 nm primary particle size (TEM), ≥99.5% trace basis.

Instrumentation

X-ray Photoelectron Spectroscopy (XPS): XPS was performed on a Kratos Axis Ultra spectrophotometers using a monochromatic Al Kα X-ray source (hv = 1486.6 eV) set at 20 mA and 15 kV, with a spot size of 700 x 300 µm², in an analysis chamber with a pressure kept below $3*10^{-9}$ mbar. The wide spectra were obtained using a pass energy of 80 eV with a step of 0.5 eV. The high-resolution core level spectra of O 1s, Ti 2p, and Cd 3d were recorded with a pass energy of 40 eV, and a measurement step of 0.1 eV. The valence band region was also measured with XPS with a similar pass energy but a lower measurement step (0.05 eV), and a higher dwell time (1500 ms). Five spectra were recorded, we verified the absence of degradation under X-ray or binding energy shift of the spectra due to the charging effect, and then we summed the spectra to maximize their signal/noise ratio.
Machine calibration was performed with sputter-cleaned Au, Cu and Ag films. The energy scale was calibrated using Au 4f7/2 at 83.96 eV and Cu 2p3/2 peaks at 932.63 eV. The overall energy resolution, as determined from the Fermi edge of an Ag reference, was 0.53 ± 0.02 eV at 40 eV pass energy. Charge neutralizer were applied on all samples. Spectra were calibrated using the Ti 2p main emission line at 458.5 eV according to a previous work.[1] The C 1s emission line from the contamination was measured at 284.9 ± 0.1 eV supporting the accuracy of our calibration method.

Data were treated using CasaXPS software.[2] A U2 Tougaard background was applied to the core levels and the area under the curves were subsequently treated with the CasaXPS_ Kratos library. For the valence band edge determination, the « edge down » background type has been used. Such mathematical function is based on the usual linear extrapolation method. To extract the CdS energy levels, we used the so-called vectorial method to our XPS spectra, described in detail.[3] The Casa XPS software has the required tools. The vectorial method is applied to the oxide (TiO_2) spectrum (S_i) and the core shell (CdS-TiO_2) one (S_f). The deduced spectra (X_j) follow the equation $X_j = (1-c_j)S_i - c_jS_f$ with c_j varying between 0 to 100 by 0.1 step scan. $X_{78.2}$ has been identified as the pure CdS spectra deduced for the TiO_2 series. A reference CdS powder (CERAC, 99.99 % purity) has been used to compare the VB spectra with the one mathematically deduced with the vectorial method.

Scanning/Transmission electron microscopy (S/TEM): Scanning/Transmission electron microscopy (S/TEM) was performed on a probe corrected S/TEM Themis Z G3 (Thermo Fisher

Scientific). The Sample was dispersed in ethanol and then deposited on a holey carbon film coated copper grid before insertion in the S/TEM. High-angle annular dark-field (HAADF-STEM) images were acquired at 300 kV, with 22 mrad convergence angle and 41-200 mrad collection angles. The Super-X system (4 Energy Dispersive X-Ray detectors) allowed acquiring elemental maps.

X-ray powder diffraction (P-XRD)

The samples were analyzed using a D8 Advance diffractometer (Bragg-Brentano geometry mode $\theta/2\theta$), equipped with a tube fitted with a copper anode. The diffractometer is equipped with a monochromator selecting the Cu Kα1 radiation (wavelength: 0.1540593 nm) and a fast silicon strip detector that simultaneously collects X-rays over a wide angular range of 3.7° in 2θ. The measurements were performed under the following conditions: X-ray tube at 40 kV voltage and 40 mA current, 3 hours per diagram, ranging from 10°2θ to 100°2θ with a step size of approximately 0.016° 2θ.

For Rietveld refinements, we used the Jana2020 program,[4] with profile functions calculated using the fundamental parameters method.[5] We used a pseudo-Voigt function for the profiles, with a Lorentzian function for broadening due to crystallite size (CSizeL parameter, in nm) and a Gaussian function for microstrains (StrainG parameter, a proportion without unity). In addition to the parameters presented in the tables, we refined the sample displacement parameter (sycos), as well as the lattice parameters of anatase and rutile (those of the CdS phases were kept fixed). To model the X-ray scattering background, we used Legendre polynomials (20 parameters, which are part of the fitting)

Gas Chromatography (GC): The gaseous reduction product, (H_2) was detected by GC analysis. In detail, using a gas-tight syringe 250 µL from the reaction headspace were injected into an Agilent 6890N GC, which was equipped with a *CARBOPLOT P7* capillary column (25 m × 0.53 mm × 25 µm) and a thermal conductivity detector (TCD). The carrier gas was Argon, and a calibration curve was initially established for H_2. Noteworthy, all the samples were also tested for aqueous products (respective aldehyde), using GC analysis as well. However, the samples were injected into Agilent 7820A GC, which was equipped with a *HP-5* capillary column (30 m × 0.32 mm × 0.25 µm). The carrier gas for the latter GC was nitrogen, and a calibration curve was established for the whole set of aldehydes screened throughout this work.

Calculation of H_2 evolution production

In every photocatalytic experiment the final amount of CdS-TiO_2 is 0.01 g. The H_2 evolution rate was calculated according to the equation:

$$\textbf{H}_2\textbf{ evolution mmol (H}_2\textbf{) g(cat)}^{-1}\textbf{ h}^{-1} = \frac{n(H_2)}{m(CAT)\ x\ t}$$

Where:

n(H_2) is the total amount of the produced H_2 (in mmol)

m(CAT) is the total amount of CdS-TiO_2 (in grams)

t is the irradiation time in hours (t = 6 h)

Synthesis and Characterizations

Preparation and characterization of CdS-TiO_2 NPs

The commercially available titanium dioxide nanoparticles (TiO_2 NPs) were immersed into a solution of $Cd(NO_3)_2$ 0.5 M in EtOH and stirred for 5 minutes at room temperature. Then, the particles were dipped into a solution of Na_2S 0.20 M in methanol/water (7:3/v:v) for additional 5 minutes under stirring. Upon each immersion, the NPs were filtered, rinsed with ethanol or methanol respectively, and dried at room temperature using a high vacuum pump. The immersion cycle was repeated four times forming the final CdS-TiO_2 NPs.

Diffuse reflectance absorption

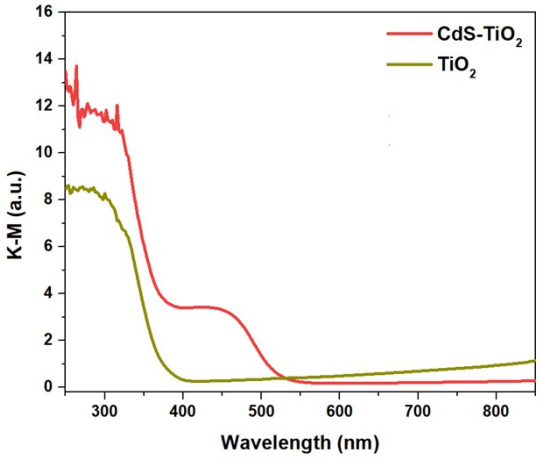

Figure S1. Kubelka-Munk transformed reflection spectra of TiO_2 and CdS-TiO_2 nanoparticles.

Emission studies

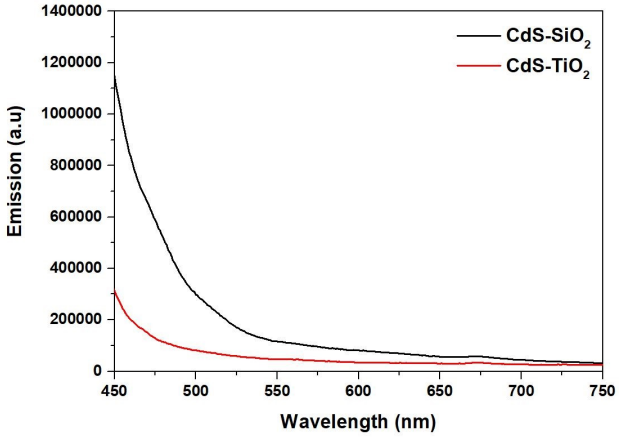

Figure S2. Emission spectra of CdS-TiO_2 (red) and CdS-SiO_2 (black) upon excitation at 410nm.

X-ray powder diffraction (P-XRD)

A)

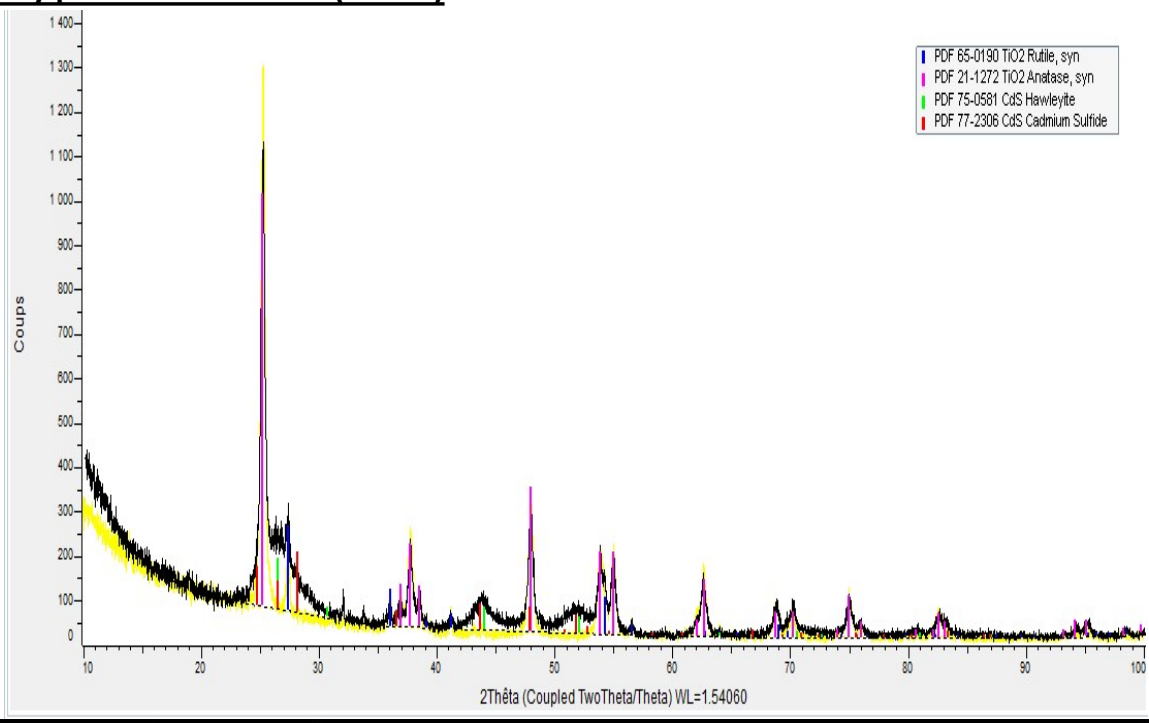

B)

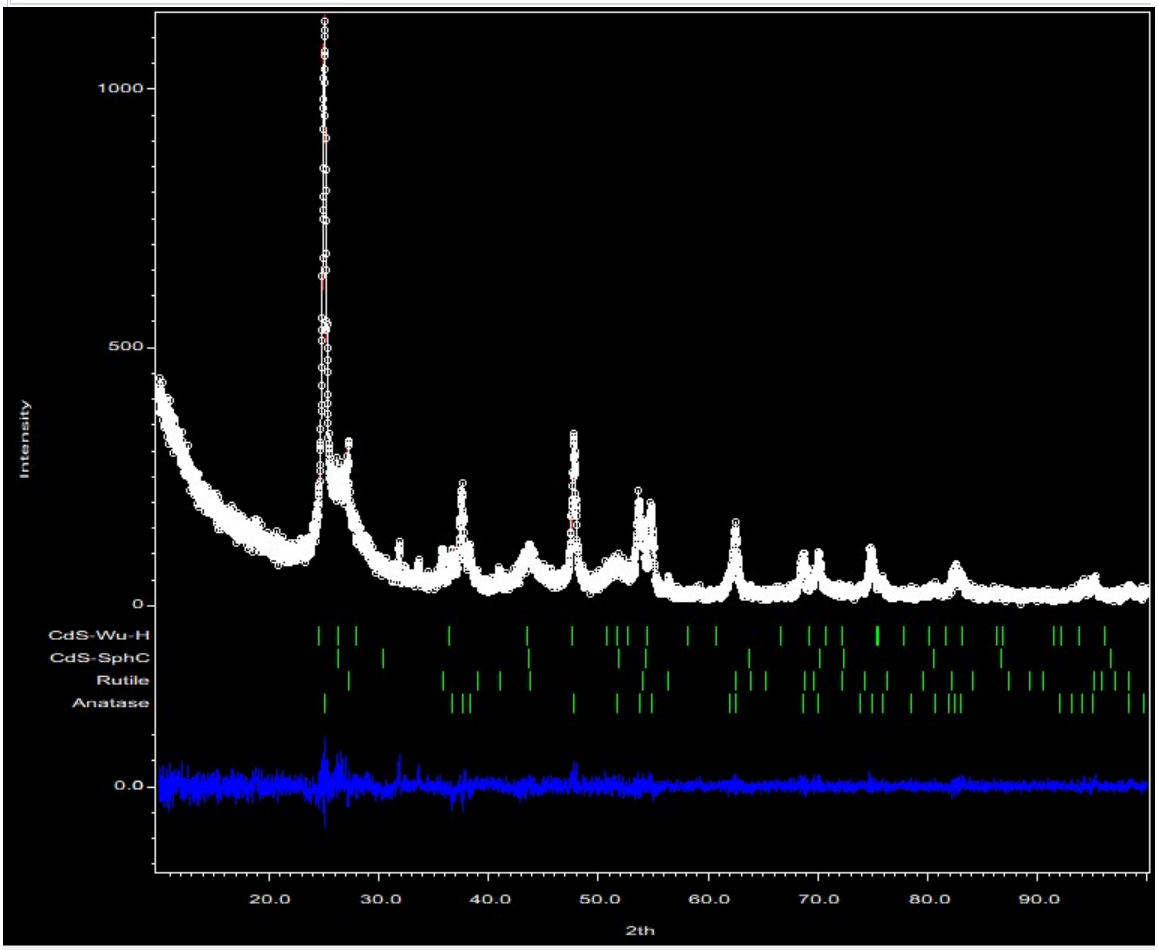

Figure S3. A) Experimental powder diffraction diagrams of of bare TiO_2 sample (black), and CdS-TiO_2 sample (yellow) with stick diagrams of Hewleyite (cubic CdS, sphalerite structure) shown in green, and those of the hexagonal CdS (wurtzite structure) shown in red and B) Rietveld refinement of CdS-TiO_2 sample, assuming that the CdS is a mixture of the cubic form (sphalerite structure) and the hexagonal form (wurtzite structure).

Table S1. Parameters from the refinement of CdS-TiO_2, assuming that the CdS is a mixture of the cubic form (sphalerite structure) and the hexagonal form (wurtzite structure). The error bar corresponds to 3*sigma multiplied by the Bérar and Lelann parameter.[6] GOF: goodness of fit. Rwp: weighted reliability factor.

Phase Name	Phase mass percentage	Size (nm)	StrainG
Anatase	58 +/-2 %	30 +/- 2	0.46 +/- 0.11
Rutile	8 +/- 1 %	49 +/- 12	0.33 (fixed)
CdS-Spha-C	20 +/- 2 %	3.4 +/- 0.2	0.001 (fixed)
CdS-Wu-H	14 +/- 2 %	3.7 +/- 0.5	0.001 (fixed)

Rwp	GOF
12.5%	1.12%

X-ray photoelectron spectroscopy (XPS)

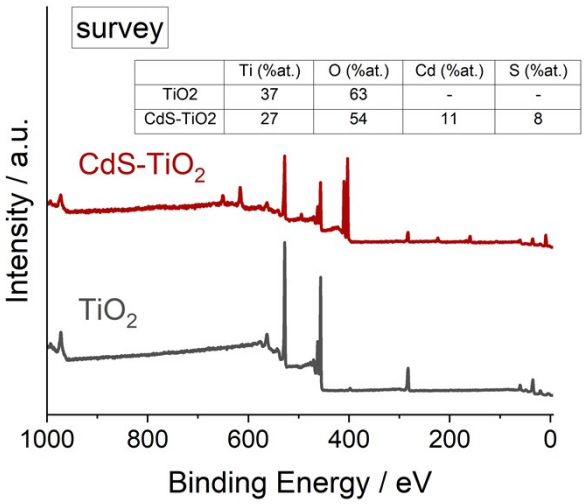

Figure S4. XPS survey spectra of TiO_2 and CdS-TiO_2 and the deduced atomic concentration

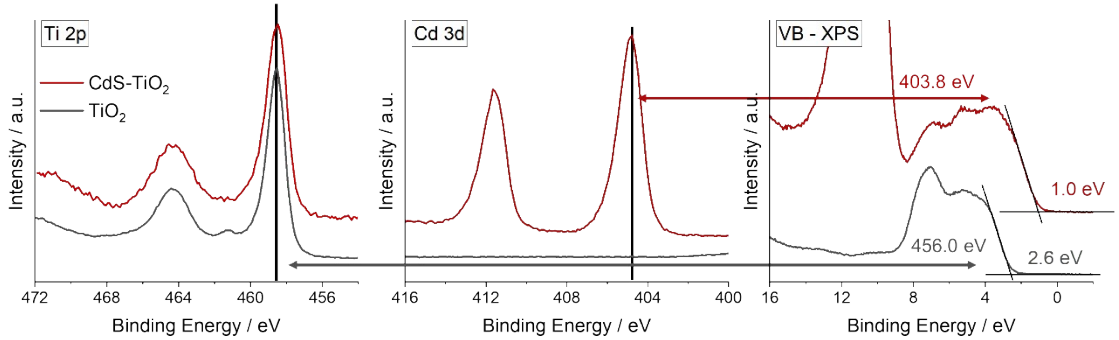

Figure S5. Core levels and valence band spectra measured by XPS for TiO_2 (black) and CdS-TiO_2 (red).

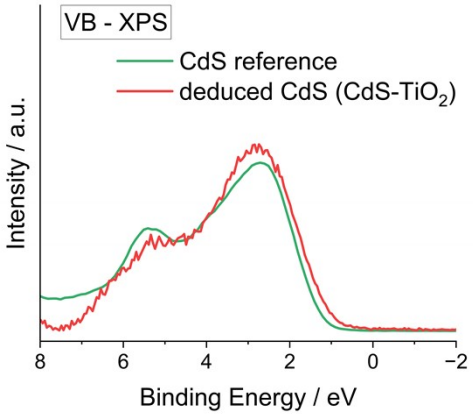

Figure S6. Valence band spectra of CdS nanopowders: the reference CdS powder (green), the spectrum obtained with the vectorial method from CdS-TiO_2 (red). Spectra were calibrated using the Cd 4d emission line at 10.8 eV and their intensity has been normalized.

Photocatalysis

DSP experiments

The experiments were performed in glass vials (20.73 mL), sealed with a rubber septum, at ambient temperature and pressure. Before each experiment, a borate buffer solution at pH = 8 was prepared, which contained 50 mM of the respective alcohol. The CdS-TiO_2 NPs (10 mg) were added in the glass vial together with 4 mL of the above-mentioned solution. The samples were degassed with Argon while being sonicated in water for 10 minutes. Finally, the samples were irradiated for 6 hours using the commercially available EvoluChem PhotoRedOxBox blue LED irradiation at 450 nm (34 mW/cm²). The amount of H_2 and aldehyde for each sample was determined using in both cases a GC instrument. In all cases, both the reported aldehyde, and H_2 values as well as the Turn Over Numbers (TONs) are the average of three independent experiments.

CdS vs. CdS-SiO_2 vs. CdS-TiO_2

We have also prepared CdS nanoparticles and compared their photocatalytic activity under the same conditions as the CdS-TiO_2 nanocomposites. For the preparation of CdS nanoparticles the hot injection method was used method.[7] The results indicate that the CdS nanoparticles do not exhibit any photocatalytic activity in these conditions. However, it is important to note that the structural and catalytic properties of CdS nanoparticles can significantly vary depending on the preparation method (e.g., SILAR *vs.* hot injection), due to differences in size, shape, and band levels.

To further clarify the role of CdS, we also developed CdS-SiO_2 nanoparticles, where SiO_2 serves as an inert support. The catalytic performances were again very low compared to those obtained with CdS-TiO_2.These studies confirmed that CdS acts primarily as a photosensitizer rather than as a photocatalyst.

Recycling experiments

The recycling experiment is illustrated in **Figure 5**, and described in the respective part of the manuscript. However, it is worth explaining why another cycle of photocatalysis (4^{th} day) could not be performed. Following the mentioned protocol (filtration, drying, etc.) approximately ~80% of the CdS-TiO_2 NPs were recovered in each cycle. Thus, at the end of the 3^{rd} cycle, we isolated approximately ~ 5 mg of the re-used CdS-TiO_2 NPs, from the initial 10 mg ones.

References

(1) Biesinger, M. C.; Lau, L. W. M.; Gerson, A. R.; Smart, R. St. C. *Resolving Surface Chemical States in XPS Analysis of First Row Transition Metals, Oxides and Hydroxides: Sc, Ti, V, Cu and Zn.* Appl. Surf. Sci. **2010**, *257* (3), 887–898. https://doi.org/10.1016/j.apsusc.2010.07.086.

(2) Fairley, N.; Fernandez, V.; Richard-Plouet, M.; Guillot-Deudon, C.; Walton, J.; Smith, E.; Flahaut, D.; Greiner, M.; Biesinger, M.; Tougaard, S.; Morgan, D.; Baltrusaitis, J. *Systematic and Collaborative Approach to Problem Solving Using X-Ray Photoelectron Spectroscopy*. Appl. Surf. Sci. Advances **2021**, *5*, 100112. https://doi.org/10.1016/j.apsadv.2021.100112.

(3) Béchu, S.; Humbert, B.; Fernandez, V.; Fairley, N.; Richard-Plouet, M. *Vectorial Method Used to Monitor an Evolving System: Titanium Oxide Thin Films under UV Illumination*. Appl. Surf. Sci. **2018**, *447*, 528–534. https://doi.org/10.1016/j.apsusc.2018.03.199.

(4) Petříček, Václav, Lukáš Palatinus, Jakub Plášil, et Michal Dušek. 2023. *Jana2020 – a New Version of the Crystallographic Computing System Jana*. *Zeitschrift Für Kristallographie - Crystalline Materials* 238 (7-8): 271-82. https://doi.org/10.1515/zkri-2023-0005.

(5) Cheary, R. W., A. A. Coelho, et J. P. Cline. 2004. *Fundamental parameters line profile fitting in laboratory diffractometers*. *Journal of Research-National Institute of Standards and Technology,* 109:1-26.

(6) Bérar, J. F., et P. Lelann. 1991. *E.s.d.'s and estimated probable error obtained in Rietveld refinements with local correlations*. *Journal of Applied Crystallography* 24 (1): 1-5. https://doi.org/10.1107/S0021889890008391.

(7) Zhang Z.; Rogers C. R.; Weiss E. A. *Energy Transfer from CdS QDs to a Photogenerated Pd Complex Enhances the Rate and Selectivity of a Pd-Photocatalyzed Heck Reaction*. J. Am. Chem. Soc. **2020**, *142*, 495−501 https://pubs.acs.org/doi/10.1021/jacs.9b11278